

**Example C**

Consider, as a last example, the rather pathological potential

$$V(r) = \begin{cases} r^{-2} \sin r^{-1}, & r < 1, \\ 0 & r > 1. \end{cases} \quad (4.16)$$

In this case, we can define  $\psi_s(k,r)$  and  $\psi_s'(k,r)$  by Eqs. (3.1) and (3.2). It can be verified that the two Born series converge, and Eqs. (3.3)–(3.6) and (1.8)

hold. Thus, for this potential, all the properties of a regular potential are obtained even though it does not satisfy Eq. (1.2).

*Note added in proof.* We want to thank Dr. M. Bég for drawing our attention to a paper by N. Limic [Nuovo Cimento **26**, 581 (1962)] which contains the statement that for singular potentials the  $S$ -matrix element for given  $l$  is the limit of the quotient of two Jost functions.

**S-Matrix Poles Close to Threshold\***

WILLIAM R. FRAZER† AND ARCHIBALD W. HENDRY

*University of California at San Diego, La Jolla, California*

(Received 13 February 1964)

Two-channel processes are studied to determine whether sizeable peaks can be produced in elastic scattering for one of the channels by threshold effects arising from the second channel (taken to be in an  $S$ -wave state). The problem is first examined by means of a simple model whose analytic properties can easily be deduced. It is found that, when all the particles are stable, large cusps occur if there is a pole of the  $S$  matrix on an unphysical sheet in the vicinity of the inelastic threshold. The cusps become “woolly” when one of the particles in the second channel is allowed to be unstable. Similar results are obtained in a calculation using an  $ND^{-1}$  formulation. These  $S$ -matrix poles correspond to virtual states of the particles in the inelastic channel, their positions on the unphysical sheets depending on the force of interaction between the particles. It is further suggested that some of the peaks observed in experiment may be of this type, having their origins in inelastic thresholds rather than direct particle resonances. In particular, the  $V_0^*$  at 1815 MeV and the  $K_1K_1$  peak near threshold may be manifestations of this.

**I. INTRODUCTION**

**M**ANY authors have discussed threshold effects, or cusps, in elementary particle reactions, including the case of a threshold for the production of an unstable particle.<sup>1-4</sup> Questions naturally arise as to whether these threshold effects can be responsible for sizeable peaks in cross sections; and if so, whether such peaks should be classified as elementary particles or as phenomena of an essentially different character. The purpose of this paper is to call attention to a situation in which threshold effects do indeed produce sizeable peaks; namely, when there exists a pole in the  $S$  matrix close to an  $S$ -wave threshold on the unphysical sheet reached by passing through the branch cut associated

with the threshold. Moreover, we conjecture that this situation is very likely to be responsible whenever a threshold effect manifests itself as a peak comparable to those associated with particles. From the point of view of  $S$ -matrix theory, a threshold effect of this nature can quite properly be called a particle since it arises from a pole in the  $S$  matrix.

In Sec. II, we shall discuss these points in more detail by considering some examples. The simplest example, given in Sec. IIA, of the type of threshold effect we are discussing is the “virtual state” occurring in the  $^1S$  state of the neutron-proton system. In Sec. IIB, the case of two channels involving only stable particles is discussed, and in Sec. IIC, two channels where one of the particles in the second channel is unstable. The latter case is an extension of the work of Nauenberg and Pais.<sup>3</sup> In Sec. III, we consider threshold effects within the framework of a dynamical model, using the matrix  $ND^{-1}$  formalism. Some clarification is thereby obtained of the work by Ball and Frazer on peaks in cross sections near the threshold for production of an unstable particle.<sup>2</sup> Lastly, in Sec. IV we discuss some possible experimental manifestations of threshold effects.

\* Work supported in part by the U. S. Atomic Energy Commission.

† Alfred P. Sloan Foundation Fellow.

<sup>1</sup> E. P. Wigner, Phys. Rev. **73**, 1002 (1948). R. Newton, Ann. Phys. (N. Y.) **4**, 29 (1958). L. Fonda and R. Newton, Phys. Rev. **119**, 1394 (1960).

<sup>2</sup> J. S. Ball and W. R. Frazer, Phys. Rev. Letters **7**, 204 (1961).

<sup>3</sup> M. Nauenberg and A. Pais, Phys. Rev. **126**, 360 (1962).

<sup>4</sup> A. Baz', Zh. Eksperim. i Teor. Fiz. **40**, 1511 (1961) [English transl.: Soviet Phys.—JETP **13**, 1058 (1961)]; Y. Fujii, Nihon University, Tokyo, Physics Department (unpublished); Y. Fujii, Progr. Theoret. Phys. (Kyoto) **29**, 71 (1963); Y. Fujii and M. Uehara, Progr. Theoret. Phys. (Kyoto) Suppl. **21**, 138 (1963).

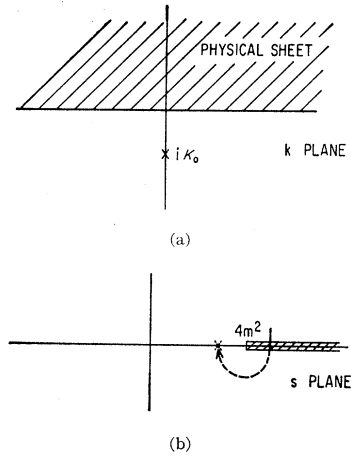


FIG. 1. The  $k$  plane and  $s$  plane with a virtual-state pole.

II. EXAMPLES OF THRESHOLD EFFECTS RESULTING FROM NEARBY POLES

A. Single-Channel Case

The most familiar example of an  $S$ -matrix pole close to a threshold on an unphysical sheet is the “virtual state” of the  $^1S$  neutron-proton system. We shall remind the reader of the nature of the singularities near threshold in this simple example because of their similarity to the more involved cases to be discussed later.

The threshold behavior of the partial-wave amplitude  $M = e^{i\delta} \sin\delta/k$ , where  $k$  is the center-of-mass momentum, is given by the scattering length formula

$$M(k) = -(1/a - ik)^{-1}. \tag{2.1}$$

The function  $M(k)$  is analytic in the complex  $k$  plane in the vicinity of  $k=0$  except for the pole at  $k=i\kappa_0$ , where  $\kappa_0=1/a$ . There are, of course, many other singularities in the complex  $k$  plane, but we are interested here only in the behavior at threshold.

The scattering length  $a$  is negative for the  $^1S$   $n$ - $p$  state ( $a \approx -23.7 \times 10^{-13}$  cm), and so the pole at  $k=i\kappa_0$  lies in the lower half-plane, as shown in Fig. 1(a). When the  $k$  plane is mapped onto the  $s$  plane, where  $s = 4(k^2 + m^2)$ , the upper-half  $k$  plane becomes the first (or physical) sheet, whereas the lower-half  $k$  plane becomes the second (or unphysical) sheet. The position of the pole on the unphysical sheet is shown in Fig. 1(b), where the arrow illustrates a path which can be followed to reach the pole from the physical region. This pole on the unphysical sheet in the  $^1S$  amplitude is often called a “virtual state.”<sup>5</sup>

In the  $^3S$  state, however, the scattering length is positive ( $a \approx 5.4 \times 10^{-13}$  cm), and the pole lies on the physical sheet. This, of course, corresponds to a bound state of the  $n$ - $p$  system, the deuteron.

Consider now the difference in the physical effects of bound and virtual states having  $\kappa_0$  equal in magnitude,

<sup>5</sup> J. M. Blatt and V. W. Weisskopf, *Theoretical Nuclear Physics* (John Wiley & Sons, Inc., New York, 1952), p. 68.

but opposite in sign. As far as the total cross section is concerned, there is no difference in the physically accessible region  $s \geq 4m^2$ . The two cases, however, are very different in the unphysical region along the real  $s$  axis below threshold in the first sheet. This region is, of course, inaccessible to experiments, but it exhibits behavior similar to that found in the two-channel case to be considered next. To evaluate the amplitude in this region, one can make the continuation  $k \rightarrow i\kappa$ , where  $\kappa$  is real and positive, and obtain the formula

$$M^{-1} = \kappa - \kappa_0. \tag{2.2}$$

The resulting function  $|M|^2$  is plotted in Fig. 2. For the bound-state case, shown below the threshold by the dashed line, there is, of course, a pole at  $s = 4(m^2 - \kappa_0^2)$ . For the virtual-state case, there is no pole but instead a large cusp at the threshold  $s = 4m^2$ . This is the type of threshold effect referred to in the Introduction, resulting from a nearby virtual-state pole.

B. Two-Channel Case, All Particles Stable

The considerations of the previous section can now be generalized to the more interesting case of threshold effects in two-channel scattering problems. We consider in this section only two-particle channels, all the particles being spinless and stable for the present. We also examine only orbital angular momentum  $L=0$  states since threshold effects are stronger in this situation.

Let  $T_{ij}$  be the partial-wave scattering matrix for the  $L=0$  state, normalized such that, in the physical region between the two thresholds,

$$T_{11}(s) = e^{i\delta_1} \sin\delta_1/k_1. \tag{2.3}$$

Here  $s$  is the square of the total energy in the center-of-mass system;  $k_1$  and  $k_2$  are the c.m. momenta in the two channels whose thresholds will be denoted by  $s_1$  and  $s_2$ , respectively.

As in the one-channel case, the threshold behavior can be seen easily from a scattering-length formula. One defines a matrix  $M$  by the equation

$$M_{ij}(s) = (T^{-1})_{ij} + ik_i \delta_{ij}. \tag{2.4}$$

It is well known, and can easily be shown to follow from the unitarity condition, that the matrix elements  $M_{ij}(s)$

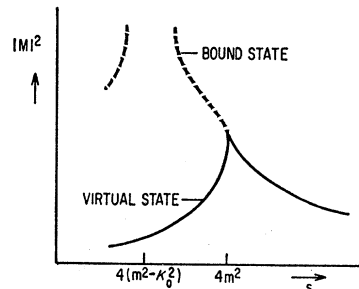


FIG. 2. The amplitude  $|M|^2$  above and below threshold for bound- and virtual-state poles.

are free from singularities at the thresholds  $s_i$ , and can therefore be expanded in a Taylor series. The scattering-length formula results from keeping only the first term; that is, the  $M_{ij}$  are taken to be real constants. Such a formula is valid, of course, only in a small region since it ignores all but the threshold singularities, but this is quite adequate for our purposes. We obtain for the  $T$  matrix

$$T_{11}(s) = (M_{22} - ik_2)/D(s), \quad (2.5a)$$

$$T_{12}(s) = -M_{12}/D(s), \quad (2.5b)$$

$$T_{22}(s) = (M_{11} - ik_1)/D(s), \quad (2.5c)$$

where

$$D(s) = (M_{11} - ik_1)(M_{22} - ik_2) - M_{12}^2. \quad (2.6)$$

In the region between the two thresholds on the real axis, it is convenient to define the real, positive quantity  $\kappa_2$  such that  $k_2 = i\kappa_2$ . Since we are interested in the effect of a pole near  $s_2$ , we require a zero of  $\text{Re}D(s)$  at a point  $s_r$  on the real axis between the thresholds. Let  $\kappa_{2r}$  be the value of  $\kappa_2$  at  $s = s_r$ . Then the condition that  $\text{Re}D(s_r) = 0$ , implies that

$$M_{11}(M_{22} + \kappa_{2r}) = M_{12}^2. \quad (2.7)$$

To cast the equations into a more familiar form, we define

$$\gamma_1 \equiv (M_{22} + \kappa_{2r}), \quad \gamma_2 \equiv M_{11}. \quad (2.8)$$

Then we obtain

$$D(s) = (\kappa_2 - \kappa_{2r})(\gamma_2 - ik_1) - i\gamma_1 k_1, \quad (2.9)$$

$$T_{11}(s) = (\gamma_1 + \kappa_2 - \kappa_{2r})/D(s), \quad (2.10a)$$

$$T_{12}(s) = -(\gamma_1 \gamma_2)^{1/2}/D(s), \quad (2.10b)$$

$$T_{22}(s) = (\gamma_2 - ik_1)/D(s). \quad (2.10c)$$

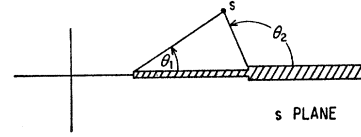
From Eq. (2.9), we see that if  $\gamma_1 \ll \gamma_2$ , there will be a pole of  $T$  near the real axis at  $\kappa_2 \approx \kappa_{2r}$ . It follows from the Schwarz reflection principle, or directly from Eq. (2.9), that there is a pair of poles, symmetric about the real axis.

We will now describe the topology of the Riemann surface of  $T$ , and investigate which sheet of this surface the pole lies on. The surface has four sheets, which can be specified as follows in terms of the angles  $\theta_1$  and  $\theta_2$  shown in Fig. 3:

$$\begin{aligned} \text{sheet I:} & \quad 0 < \theta_1 < 2\pi, \\ & \quad 0 < \theta_2 < 2\pi; \\ \text{sheet II:} & \quad 2\pi < \theta_1 < 4\pi, \\ & \quad 0 < \theta_2 < 2\pi; \\ \text{sheet III:} & \quad 2\pi < \theta_1 < 4\pi, \\ & \quad 2\pi < \theta_2 < 4\pi; \\ \text{sheet IV:} & \quad 0 < \theta_1 < 2\pi, \\ & \quad 2\pi < \theta_2 < 4\pi. \end{aligned} \quad (2.11)$$

We have attempted to depict these four sheets in Fig. 4, where we show three cross sections of the

FIG. 3. The  $s$  plane with elastic and inelastic cuts.



Riemann surface. All four sheets join at the branch point  $s_2$ . Note that, except at this point, sheet IV has no direct connection to the physical region.

One can easily determine on which sheet of  $D(s)$  the zeros lie. This is outlined in the Appendix. It is shown there that poles close to the real axis in the vicinity of the inelastic threshold cannot occur in sheets I or III, but lie in sheets II or IV.

The case of a pole in sheet II close to  $s_2$  was studied by Dalitz and Tuan for the  $\pi Y, KN$  system.<sup>6</sup> This pole was given the name "KN bound state."<sup>7</sup> In general, we shall refer to a pole in sheet II near  $s_2$  as a bound state of the particles in channel 2. Since sheet II is directly accessible from the physical region for  $s_1 < s < s_2$ , a pole on this sheet manifests itself as a resonance in the channel 1 scattering process.

On the other hand, a pole in sheet IV manifests itself in a manner analogous to the virtual state discussed in Sec. IIA; namely, as a large cusp at  $s_2$ . We shall refer to a pole in sheet IV close to  $s_2$  as a virtual state of the particles in channel 2.<sup>7</sup>

Examples of the two cases are shown in Fig. 5, and the corresponding path of the pole as  $\kappa_{2r}$  is varied is drawn in Fig. 6. We have illustrated the situation by using the channels  $\pi + N$  and  $\rho + N$  with the  $\rho$  meson stable. In the figures, the inelastic threshold is therefore at  $(W - M) = m_\rho = 5.4m_\pi$ . A pole in sheet IV produces a cusp in channel 1 scattering at the energy  $s_2$ . The height of the cusp increases as the pole position is taken closer to the real axis in sheet IV. As the pole crosses the real axis (just above  $s_2$ ) and moves into sheet II, the cusp attains the unitarity limit and becomes a rounded resonance peak whose position changes as the pole moves away from  $s_2$  in sheet II.

We have also drawn in Fig. 5 the corresponding in-

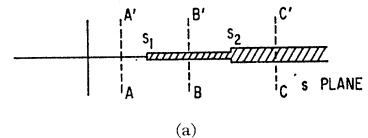
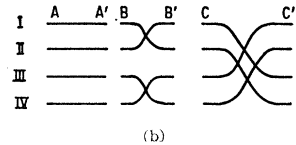


FIG. 4. The four sheets of  $T_{ij}(s)$  and their interconnection on crossing the real  $s$  axis.



<sup>6</sup> R. Dalitz and S. Tuan, Ann. Phys. (N. Y.) **10**, 307 (1960).  
<sup>7</sup> Dalitz and Tuan (Ref. 6) in fact used the name "virtual bound state." We drop the word "virtual" since we wish to use it in the sense in which it is used in Ref. 5 and Sec. IIA of this paper.

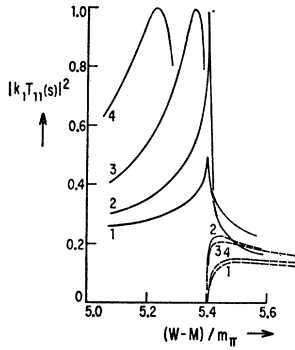


FIG. 5. Cusps and resonance peaks (solid lines) for the elastic amplitude  $|k_1 T_{11}(s)|^2$ ; the dashed lines are the corresponding inelastic contributions  $k_1 k_2 |T_{12}(s)|^2 = \frac{1}{4}(1-\eta^2)$  with  $0 \leq \eta \leq 1$ . The parameters have the values  $\gamma_1 = 1.0$ ,  $\gamma_2 = 10.0$ , while  $\kappa_{2r} = -0.7, -0.1, 0.5$ , and  $1.0$  for the cases indicated by 1, 2, 3, 4, respectively. Peaks 3, 4 attain their elastic unitarity limit 1.0.

elastic contribution  $k_1 k_2 |T_{12}|^2 = \frac{1}{4}(1-\eta^2)$ , where unitarity imposes the restriction  $0 \leq \eta \leq 1$ . There is a rapid square root rise for energies just above the inelastic threshold.

To avoid possible confusion, we conclude this section by comparing the model just discussed with the models advanced in criticisms of the work of Oakes and Yang<sup>8</sup> by a number of authors.<sup>9</sup> These authors found that resonance poles near inelastic thresholds may occur in more than one sheet, whereas the case we discuss involves a conjugate pair of poles on one sheet only. The difference lies in our having taken the  $M_{ij}$  as real constants, whereas in the model of Dalitz and Rajasekaran,<sup>9</sup> for example, the  $M_{ij}$  have a zero associated with the resonance. The distinction between these two cases has been made quite explicitly by Dalitz.<sup>10</sup>

### C. Two-Channel Case, One Particle Unstable: Woolly Cusp

The way to generalize the formulas of the preceding section to the case where an unstable particle is produced has been pointed out by Nauenberg and Pais,<sup>3</sup> and by Ball, Frazer, and Nauenberg.<sup>11</sup> To make the notation more tractable, we deal with a particular example, namely the two channels  $\pi+N$  and  $\pi+\pi+N$  in which the two pions emerge as a  $\rho$  meson. The  $S_{1/2}$  and  $D_{3/2}$  states of the pion-nucleon system are the interesting ones, since it is those which couple to a  $\rho-N$  state of zero orbital angular momentum. Here, in order to illustrate the calculations simply, we consider only the  $S_{1/2}$  state, leaving the more realistic  $D_{3/2}$  situation to Sec. IV. The only change needed in the preceding formalism is the replacement of  $k_2$  by the appropriate phase-space factor for a  $\rho N$  state, given in Eq. (3.9) of

Ref. 11, that is  $k_2(s) \rightarrow \rho_2(s, \gamma_\rho)$  where

$$\rho_2(s, \gamma_\rho) = \frac{1}{\pi} \int_{4m_\pi^2}^{\infty} d\sigma k_2(s, \sigma) \left[ \frac{(\sigma-4)^3 - 1/2}{\sigma} \right] \times \frac{1/2 \gamma_\rho}{(m_\rho^2 - \sigma)^2 + \gamma_\rho^2 (\sigma-4)^3 / 4\sigma}, \quad (2.12)$$

and where  $k_2(s, \sigma)$  is the center-of-mass momentum of a nucleon and a particle of mass  $\sqrt{\sigma}$ ,

$$[k_2(s, \sigma)]^2 = [\sigma - (W+m)^2][\sigma - (W-m)^2] / 4s, \quad (2.13)$$

with  $W = s^{1/2}$ . Actually,  $\rho_2(s, \gamma_\rho)$  differs from Eq. (3.9) of Ref. 8 in that here the upper limit is  $\infty$ . As discussed by Nauenberg and Pais, this corresponds to the absence of  $\theta$  functions in the  $k_i$  of Eq. (2.4).<sup>3</sup>

Although the integral over  $\sigma$  in Eq. (2.12) is formally divergent, it is to be interpreted in the sense that only the contribution of the  $\rho$ -meson peak is to be included. We are attempting to include only that portion of the  $\pi\pi N$  state in which the two pions are produced as a  $\rho$  meson.

Nauenberg and Pais have observed that for a narrow resonance ( $\gamma_\rho \ll 1$ ), one can reduce  $\rho_2(s, \gamma_\rho)$  to a simple approximate form valid in the region around  $W = m + m_\rho$  by setting  $\sigma = m_\rho$  in those factors of (2.12) which are slowly varying and letting the lower limit go to  $-\infty$ . One thus obtains

$$\rho_2(s, \gamma_\rho) \approx [k_2(s, m_\rho^2) + i\delta]^{1/2} \quad (2.14)$$

$$= \left[ \frac{1}{2} ((k_2^4 + \delta^4)^{1/2} + k_2^2) \right]^{1/2} + i \left[ \frac{1}{2} ((k_2^4 + \delta^4)^{1/2} - k_2^2) \right]^{1/2}, \quad (2.15)$$

where  $\delta$  is given by

$$\delta = [2mm_\rho / (m + m_\rho)] \Delta, \quad (2.16)$$

and  $\Delta$  is the half-width of the  $\rho$  meson. Unfortunately, the narrow-width approximation is not very good for the  $\rho$  (or even, we find, for the  $K^*$ ), so we shall continue to use Eq. (2.12), evaluated numerically, in the examples we present.

From Eq. (2.12), we can easily see that there is a branch point of  $\rho_2$ , and hence of  $T_{ij}$ , at  $s = (m + 2m_\pi)^2$ . Of more interest is the branch point associated with  $\rho$  production at  $s = s_\rho$ , where  $s_\rho = (m + m_\rho - i\Delta)^2$ , which can most easily be identified in Eq. (2.14). The existence

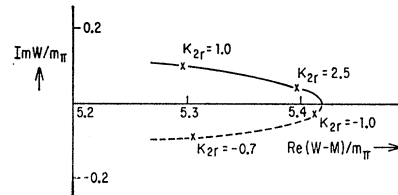


FIG. 6. Path of the pole in sheets II (solid line) and IV (dashed line) as  $\kappa_{2r}$  is varied, with  $\gamma_1 = 1.0$  and  $\gamma_2 = 10.0$ . The path of the simultaneous complex conjugate pole is not marked. The inelastic threshold occurs at  $(W-M)/m_\pi = m_\rho/m_\pi = 5.4$ .

<sup>8</sup> R. J. Oakes and C. N. Yang, Phys. Rev. Letters **11**, 174 (1963).

<sup>9</sup> D. Amati, Phys. Letters **7**, 290 (1963); R. H. Dalitz and G. Rajasekaran, Phys. Letters **7**, 373 (1963); R. J. Eden and J. G. Taylor, Phys. Rev. Letters **11**, 516 (1963); M. Nauenberg and J. C. Nearing, *ibid.* **12**, 63 (1963); M. Ross, *ibid.* **11**, 450 (1963).

<sup>10</sup> R. H. Dalitz, Rev. Mod. Phys. **33**, 471 (1961). See, also, p. 475, articles (a) and (b).

<sup>11</sup> J. Ball, W. Frazer, and M. Nauenberg, Phys. Rev. **128**, 478 (1962).

of this threshold was first pointed out by Blankenbecler, Goldberger, MacDowell, and Treiman,<sup>12</sup> and has recently been demonstrated more rigorously within the framework of  $S$ -matrix theory by Zwanziger<sup>13</sup> and by Gunson.<sup>14</sup> In the remainder of this section, we shall discuss the effects of  $S$ -matrix poles near this threshold. The relevant branch cuts of  $T_{ij}(s)$  are shown in Fig. 7. The branch point at  $s=s_\rho$  lies on the sheet reached by continuing from the physical region in the vicinity of  $s=m_\rho^2$  down into the lower half-plane. In analogy to the case discussed in the previous section, we designate this as sheet III. If one then continues on through the cut starting at  $s_\rho$ , one reaches another sheet which we shall call sheet III'. The fact that there is a conjugate branch point at  $(m+m_\rho+i\Delta)^2$  follows directly from Eq. (2.12), or from the Schwarz reflection principle.

By analogy with the two-channel, stable-particle case discussed previously, we shall call a pole lying near  $s_\rho$  in sheet III a  $\rho N$  bound state, and in sheet III' a  $\rho N$  virtual state. The  $\rho N$  bound-state pole appears in the physical region as an ordinary resonance since sheet III is directly accessible from the physical region, whereas the virtual-state pole produces a large "woolly cusp," somewhat different in shape.<sup>15</sup>

FIG. 7. The  $s$  plane with the branch points on sheet III at  $s=(m+m_\rho\pm i\Delta)^2$  arising from the unstable  $\rho$  meson.

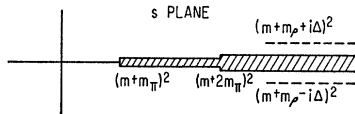


Figure 8 shows how, as the pole on sheet III' moves towards the branch point at  $s_\rho$  and passes into sheet III, a woolly cusp grows at the inelastic threshold, eventually reaching the unitarity limit and moving to the left as a resonance. The inelastic contribution is likewise smoothed out. The extent of the woolliness of course depends on the unstable  $\rho$ -meson width, and this is demonstrated in Fig. 9 where several values of  $\gamma_\rho$  were been considered.

We have thus shown that the  $\rho N$  virtual-state pole produces a woolly cusp which can be high and narrow enough to be comparable with more conventional unstable particle peaks. But in this case, which we feel is the only case in which a woolly cusp will attain such proportions, the woolly cusp is not a phenomenon essentially different from the ordinary resonance. The only difference, as we shall discuss in the next section, is that in the virtual-state case the forces are slightly

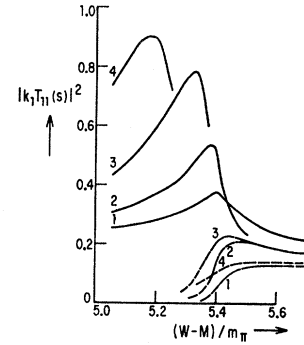
<sup>12</sup> R. Blankenbecler, M. Goldberger, S. MacDowell, and S. Treiman, Phys. Rev. **123**, 692 (1961).

<sup>13</sup> D. Zwanziger, Phys. Rev. **131**, 888 (1963).

<sup>14</sup> J. Gunson, University of Birmingham, November 1962 (unpublished).

<sup>15</sup> Although we follow Nauenberg and Pais very closely in this section, one difference should be noted. Our formulas are essentially the same down to their Eq. (2.35) of Ref. 3. Following this equation, they make an approximation which is invalid in the case of interest to us here, the virtual-state case.

FIG. 8. Elastic peaks with corresponding inelastic contributions for an unstable  $\rho$  meson with narrow width  $\gamma_\rho=0.02$ . The parameters are  $\gamma_1=1.0$ ,  $\gamma_2=10.0$ , and  $\kappa_{2r}=-0.7, -0.1, 0.5, 1.0$  for the cases 1, 2, 3, 4, respectively. In the figure, peaks 3, 4 attain their unitarity limits.



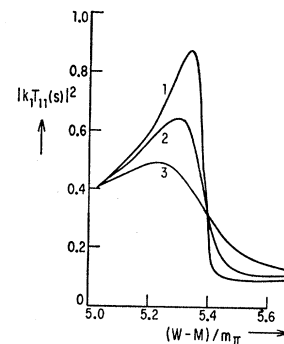
weaker than in the bound-state case. This would not seem to be a sufficient reason for making a fundamental distinction. A pole which manifests itself as a woolly cusp certainly seems entitled to be placed on a Regge trajectory, or included in any other classification scheme for the elementary particles. Similar remarks apply to the mechanism proposed by Ball and Frazer in connection with the higher resonances in pion-nucleon scattering,<sup>2</sup> but we shall defer a detailed discussion to the next section.

### III. BOUND AND VIRTUAL STATES IN THE $ND^{-1}$ FORMALISM

In this section we shall re-examine within the matrix  $T=ND^{-1}$  formalism the bound- and virtual-state poles discussed in Sec. II. The purpose is to investigate the motion of the pole as the nature and strength of the force is varied. The case of a strong force in an off-diagonal channel is particularly interesting, since it was pointed out by Ball and Frazer that the force arising from one-pion exchange in the reaction  $\pi+N \rightarrow \rho+N$  is very strong in the  $\pi N D_{3/2}$  state. This strong force is undoubtedly influential in producing the  $N_{1/2}^*$  at 1512 MeV.

For the sake of illustration, we shall again outline our procedure using the channels  $\pi+N$  and  $\rho+N$ , taken in  $D$ - and  $S$ -wave orbital angular momentum states, respectively. The  $ND^{-1}$  equations have been derived in Ref. 11 and also by Cook and Lee.<sup>16</sup> In

FIG. 9. Variation of peak width for different values of the  $\rho$ -meson width. The peaks have  $\gamma_1=1.0$ ,  $\gamma_2=10.0$ ,  $\kappa_{2r}=0.5$ , and  $\gamma_\rho=0.01, 0.05, 0.15$  for cases 1, 2, 3, respectively.



<sup>16</sup> L. F. Cook and B. W. Lee, Phys. Rev. **127**, 283 and 297 (1962).

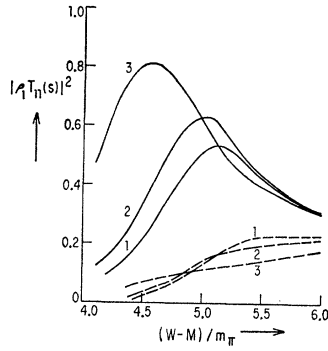


FIG. 10. Elastic peaks and corresponding inelastic contributions with only the off-diagonal interaction. Here  $\gamma_\rho = 0.33$ ,  $R_{11} = 0$ ,  $R_{22} = 0$ ,  $s_{12} = -400m_\pi^2$ , and the residue  $R_{12}$  has the values  $R_{12} = 3.2 \times 10^4$ ,  $3.4 \times 10^4$ ,  $3.8 \times 10^4$  for cases 1, 2, 3, respectively. Peak 3 attains its unitarity limit.

addition, we shall make the greatly simplifying approximation of representing the left-hand cuts in each reaction by a single pole term, of the form  $R_{ij}/(s-s_{ij})$ .<sup>17</sup>

Let us start by considering only the effect of the off-diagonal interaction  $R_{12}$ , that is, take  $R_{11} = 0 = R_{22}$ . The equations for  $N$  and  $D$  reduce to

$$\begin{aligned} N_{11}(s) &= R_{12}D_{21}(s_{12})/(s-s_{12}), \\ N_{12}(s) &= R_{12}D_{22}(s_{12})/(s-s_{12}), \\ N_{21}(s) &= R_{12}D_{11}(s_{12})/(s-s_{12}), \\ N_{22}(s) &= R_{12}D_{12}(s_{12})/(s-s_{12}), \end{aligned} \quad (3.1)$$

and

$$\begin{aligned} D_{11}(s) &= 1 - R_{12}D_{21}(s_{12})U(s, s_{12}), \\ D_{12}(s) &= -R_{12}D_{22}(s_{12})U(s, s_{12}), \\ D_{21}(s) &= -R_{12}D_{11}(s_{12})V(s, s_{12}), \\ D_{22}(s) &= 1 - R_{12}D_{12}(s_{12})V(s, s_{12}), \end{aligned} \quad (3.2)$$

where  $U, V$  are the integrals

$$\begin{aligned} U(s, s_{ij}) &= \frac{1}{\pi} \int_{(M+m_\pi)^2}^{\infty} ds' \frac{\rho_1(s')}{(s'-s)(s'-s_{ij})}, \\ V(s, s_{ij}) &= \frac{1}{\pi} \int_{(M+2m_\pi)^2}^{\infty} ds' \frac{\rho_2(s')}{(s'-s)(s'-s_{ij})}. \end{aligned}$$

The phase-space factors  $\rho_i(s)$  are taken to be<sup>18</sup>

$$\rho_1(s) = \frac{1}{8\pi} \left( \frac{k_1(s)}{\sqrt{s}} \right)^6$$

<sup>17</sup> It may be noted that, in nonrelativistic potential scattering, a pole term on the left corresponds to an Eckart potential in the Schrödinger equation [V. Bargmann, Rev. Mod. Phys. **21**, 488 (1949)]. For large distances, an Eckart potential behaves as a Yukawa potential.

<sup>18</sup> By taking  $\rho_1(s)$  of the form indicated, we have introduced through the  $1/s^2$  factor two extra poles at the origin. This factor however is necessary in order to make the integrals  $U(s, s_{ij})$  convergent for a  $D$ -wave  $\pi+N$  state. These extra poles, which are required to compensate for the factor  $2l+1$ , may be regarded as representing the "centrifugal barrier" interaction.

and

$$\begin{aligned} \rho_2(s) &= \frac{1}{\pi} \int_{4m_\pi^2}^{(\sqrt{s}-M)^2} d\sigma \frac{k_2(s, \sigma)}{\sqrt{s}} \left[ \frac{(\sigma - 4m_\pi^2)^3}{\sigma} \right]^{-1/2} \\ &\quad \times \frac{\frac{1}{2}\gamma_\rho}{(m_\rho^2 - \sigma)^2 + \gamma_\rho^2(\sigma - 4m_\pi^2)^3/4\sigma}, \end{aligned}$$

where  $k_2(s, \sigma)$  is expressed in (2.13), and a Breit-Wigner formula has again been used to describe the unstable spin-1  $\rho$  meson. We have  $m_\rho = 5.4m_\pi$ , and a  $\rho$  width of 100 MeV yields  $\gamma_\rho \approx 0.33$ .

The above equations were evaluated numerically with various values of  $s_{12}$  and  $R_{12}$ , care being taken to avoid ghosts.<sup>19</sup> The most noticeable feature coming out of the calculations is the behavior of the elastic scattering amplitude  $T_{11}(s)$  as the residue  $R_{12}$  is increased: a peak in  $|\rho_1 T_{11}(s)|^2$  gradually develops in the vicinity of the threshold energy  $s \approx (M+m_\rho)^2$ . For values of  $R_{12}$  less than a certain value  $R_t$  (with  $s_{12}$  held fixed), none of the corresponding peaks attain the maximum heights allowed by unitarity; while for  $R_{12}$  greater than  $R_t$ , the peaks do reach their unitarity limits and move to the left with increasing  $R_{12}$ . This is illustrated in Fig. 10, where we have also drawn the inelastic contributions  $\rho_1 \rho_2 |T_{12}|^2$ .

The  $ND^{-1}$  equations (3.1) and (3.2) can easily be generalized to incorporate the diagonal terms  $R_{11}$  and  $R_{22}$ . It was found that a peak for fixed  $R_{12}$  was not affected much by  $R_{11}$  (taken sufficiently small so as not to give rise to a direct resonance in the  $T_{11}$  amplitude). On the other hand,  $R_{22}$  had quite an appreciable influence. Increasing  $R_{22}$  has a similar effect to increasing  $R_{12}$ , as indicated in Fig. 11.

These results are analogous to those obtained in Sec. IIC, and it seems very likely that the peaks in the above  $ND^{-1}$  formulation have a similar origin to those in Sec. II. The residues  $R_{12}$  and  $R_{22}$  represent the force of interaction in the  $\rho+N$  state. As this force gradually

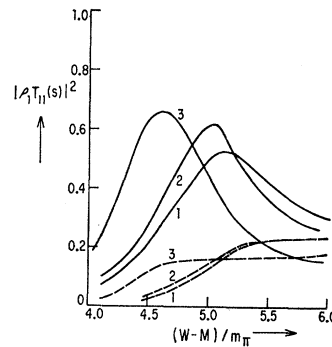


FIG. 11. Elastic peaks and corresponding inelastic contributions with  $\gamma_\rho = 0.33$ ,  $R_{11} = 0$ ,  $s_{12} = -400m_\pi^2$ ,  $R_{12} = 3.2 \times 10^4$ ,  $s_{22} = 0$ , and  $R_{22} = 0, 33, 130$  for cases 1, 2, 3, respectively. Peak 3 attains its unitarity limit.

<sup>19</sup> For  $R_{12}$  sufficiently large, namely  $R_{12} > [U(s_{12}, s_{12})V(s_{12}, s_{12})]^{-1}$ , the matrix elements  $T_{ij}(s)$  develop a spurious pole singularity which moves in from the left along the negative real  $s$  axis as  $R_{12}$  is increased. This corresponds to a "ghost" and not to a bound state, since its binding energy is initially infinite and then becomes smaller as the interaction  $R_{12}$  is taken larger.

becomes stronger (increasing  $R_{12}$ ,  $R_{22}$ ), a pole corresponding to a  $\rho N$  virtual state approaches the branch point at  $s = (M + m_\rho + i\Delta)^2$  on sheet III', producing a woolly cusp in the elastic-scattering cross section. Simultaneously of course a complex conjugate pole approaches  $s = (M + m_\rho - i\Delta)^2$ . For a sufficiently strong force, the pole moves through to sheet III, forming a real  $\rho N$  bound state. At all stages, the height and position of the peak depends on the position of the pole: the latter in turn depends on the force of interaction between the  $\rho$  meson and the nucleon.

The model considered above permits us to gain further insight into the nature of the phenomenon investigated by Ball and Frazer.<sup>2</sup> These authors found that a sufficiently rapidly rising inelastic amplitude (such as at the threshold for  $\pi + N \rightarrow \rho + N$ ) would produce a peak in the elastic scattering. Equation (3) of their paper is applicable to the above model as long as  $R_{11} = 0$ . In Fig. 10, case 1, one sees a peak associated with an inelastic amplitude which rises rapidly to nearly the unitarity limit.<sup>20</sup> In the Ball-Frazer treatment, it was not clear whether such a peak was associated with a pole in the  $S$  matrix, whereas in the present model this is indeed the case. It follows also from Fig. 9 that such a peak is the same phenomenon as the "woolly cusp" of Nauenberg and Pais,<sup>3</sup> since the peak degenerates into an ordinary cusp as the width of the  $\rho$  meson is decreased to zero.

Moreover, we believe that these conclusions are quite general. The formulas we have used in this and the preceding section should provide an adequate representation of the scattering amplitudes in a small region around the production threshold.

#### IV. POSSIBLE EXPERIMENTAL MANIFESTATIONS

In the preceding sections, we have demonstrated how an elastic-scattering process may have a sizeable peak due to the effect of an inelastic channel when there is a bound or virtual state of the inelastic channel in the vicinity of its threshold. Simultaneously, there is a rapid rise in the cross section for the inelastic reaction. It is natural to ask therefore whether any of the many peaks in the experimental data are of this type. We discuss some possible candidates.

##### A. The $K_1 K_1$ Threshold Anomaly

It has been observed experimentally that the cross section for the reaction  $\pi + \pi \rightarrow K + \bar{K}$  in the  $I=0$ ,  $S$ -wave state is large just above its threshold<sup>21</sup>: this

<sup>20</sup> In cases 2 and 3 of Fig. 9, one sees that, as the strength  $R_{12}$  of the interaction is increased and the peak moves away from the  $\rho N$  threshold, the magnitude of the inelastic amplitude just above threshold decreases. Equation (3) of Ball and Frazer is still valid for this situation, but the peak is no longer directly associated with a rapidly rising inelastic cross section.

<sup>21</sup> A. R. Erwin, G. A. Hoyer, R. H. March, W. D. Walker, and T. P. Wangler, Phys. Rev. Letters **9**, 34 (1962); **10**, 204(E) (1963); G. Alexander, O. I. Dahl, L. Jacobs, G. R. Kalbfleisch, D. H. Miller, A. Rittenberg, J. Schwartz, and G. A. Smith, *ibid.* **10**, 460

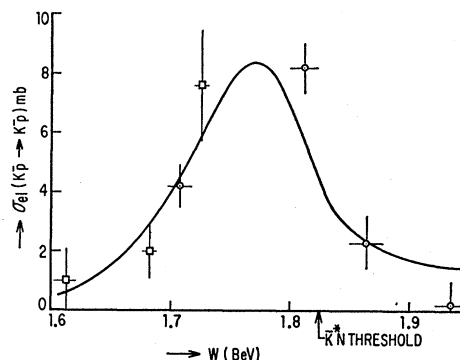


FIG. 12. Cross section for  $J = \frac{3}{2}^- K^- p$  scattering with  $\gamma_1 = 1.0$ ,  $\gamma_2 = 0.025$  and  $\kappa_{2r} = 0.09$ . Total width of  $\bar{K}^*$  is taken as 50 MeV. Experimental points are those of Bastien *et al.* ( $\square$ ) and Sodickson *et al.* ( $\circ$ ) (Ref. 21) with a background subtraction of 15 mb.

probably corresponds to the situation where there is a pole close to the  $K\bar{K}$  threshold. Unfortunately, the data for both this inelastic reaction and elastic  $\pi\pi$  scattering at these energies is as yet too inaccurate to determine whether this effect might be due to a virtual state of the  $K_1 K_1$  system, or a bound state. The two cases are easy to distinguish if the pole is not too close to the  $K\bar{K}$  threshold: the bound-state pole appears as a peak at the pole position in elastic  $\pi\pi$  scattering; the virtual-state pole is observable only as a threshold anomaly.

It seems to us that there is no reason to regard a virtual state as less fundamental than any other entries in the list of elementary particles. The only criterion available to us, on the basis of present theories, for deciding whether a peak in a cross section should be called a particle is whether or not it is associated with a pole in the  $S$  matrix. Neither a virtual-state pole nor an ordinary resonance pole is on the physical sheet, but this is not usually regarded as a fundamental distinction.

##### B. The $N_{1/2}^*$ (1512 MeV)

It was suggested by Ball and Frazer<sup>2</sup> that the  $D_{3/2}$  second pion-nucleon resonance  $N_{1/2}^*$  at 1512 MeV might be associated with the opening of the  $\rho$ -production channel. This idea has been developed by several authors.<sup>11,16,22</sup> Since the one-pion exchange force in the off-diagonal channel reaction  $\pi + N \rightarrow \rho + N$  is very strong, it seems likely that this mechanism plays an essential role in the formation of the  $N_{1/2}^*$ . It is clear however from the fact that the  $\rho N$  threshold lies around 1690 MeV, that the  $N_{1/2}^*$  must be a  $\rho N$  bound state, rather than a  $\rho N$  virtual state. (The distinction between an ordinary elastic resonance and a bound state of the

(1963); A. Bigi, S. Brandt, R. Carrara, W. A. Cooper, A. de Marco, G. R. MacLeod, Ch. Peyrou, R. Sosnowski, and A. Wroblewski, *Proceedings of the 1962 International Conference on High Energy Physics* (Interscience Publishers, Inc., New York, 1962), p. 247.

<sup>22</sup> V. Teplitz, thesis, University of Maryland, 1962 (unpublished); U. Amaldi, Jr., and F. Selleri, *Nuovo Cimento* (to be published).

inelastic channel is not a sharp one, but the latter terminology is sometimes useful.)

### C. The $Y_0^*$ (1815 MeV)

In  $K$ -meson-nucleon scattering, the  $Y_0^*$  peak at 1815 MeV lies very close to the  $\bar{K}^*N$  threshold.<sup>23</sup> Moreover, Ball and Frazer pointed out that the one-pion exchange process for  $\bar{K}^*$  production is very strong in the  $I=0$  state. These facts suggest that the  $Y_0^*$  be interpreted as a virtual, or just barely bound, state of the  $S$ -wave  $\bar{K}^*N$  system.<sup>24,25</sup> This would require the  $Y_0^*$  to be a  $D_{3/2}$  resonance in the  $K^- + p$  channel.

The quantum numbers of this peak, however, have not yet been firmly established. The height of about 8 mb above a background of about 15 mb, observed in elastic  $K^-p$  scattering, requires  $J \geq \frac{3}{2}$ . The angular distributions have been measured by Beall *et al.* and by Sodickson *et al.*,<sup>26</sup> who find a large  $(\cos\theta)^5$  term. This has led some authors<sup>27</sup> to conclude that  $J = \frac{5}{2}$ ; however, the possibility of a resonant  $D_{3/2}$  combined with background terms including a small  $F_{7/2}$  seems quite consistent with the data available at present.<sup>28</sup>

In Fig. 12, we have drawn an approximate fit to the experimental data (with a 15 mb background subtraction) using the model described in Sec. IIC. The phase-space factors were taken as  $(k_1/\sqrt{s})^5$  for the  $D_{3/2}$   $\bar{K}N$  channel, and  $k_2(s, \sigma)/\sqrt{s}$  for the  $S$ -wave  $\bar{K}^*N$  channel, while a total width of 50 MeV was used for the  $\bar{K}^*$ . The slight asymmetry of the observed peak lends further support to the hypothesis that the peak is strongly affected by the  $\bar{K}^*N$  threshold.<sup>26,27</sup>

### ACKNOWLEDGMENTS

The authors would like to thank Dr. J. S. Ball, Dr. M. Nauenberg, and Dr. P. G. Thurnauer for

<sup>23</sup> O. Chamberlain, K. M. Crowe, D. Keefe, L. T. Kerth, A. Lamonick, T. Muang, and T. F. Zipf, *Phys. Rev.* **125**, 1696 (1962).

<sup>24</sup> The objection has frequently been raised that the one-pion exchange force for  $K^*$  production in  $K^+N$  scattering in the  $I=0$  state is equally strong, but no large peak is seen in  $K^+n$  scattering at this threshold [V. Cook, D. Keefe, L. T. Kerth, *et al.*, *Phys. Rev. Letters* **7**, 182 (1961)]. The forces acting in the  $KN$  and  $\bar{K}N$  channels are quite different, however; moreover, there are many more inelastic channels available to the  $\bar{K}N$  system. One should therefore not be surprised if the  $K^*N$  threshold behavior is quite different in the two channels.

<sup>25</sup> This model has been considered further by Chia Hwa Chan, Imperial College, London (unpublished).

<sup>26</sup> E. F. Beall, W. Holley, D. Keefe, L. T. Kerth, J. J. Thresher, C. L. Wang, and W. A. Wenzel, *Proceedings of the 1962 International Conference on High Energy Physics* (Interscience Publishers, Inc., New York, 1962) p. 368; P. L. Bastein, J. P. Berge, O. I. Dahl, M. Ferro-Luzzi, J. Kirz *et al.*, *ibid.*, p. 373; L. Sodickson, Y. Manelli, D. Frisch, and M. Wahlig, MIT Physics Department (unpublished).

<sup>27</sup> S. L. Glashow and A. H. Rosenfeld, *Phys. Rev. Letters* **10**, 192 (1962), tentatively assign the  $Y_0^*$  (1815 MeV) to a  $\frac{5}{2}^+$  octet in the unitary symmetry scheme.

<sup>28</sup> W. A. Wenzel and L. Sodickson (private communications).

many valuable discussions during the course of this work.

### APPENDIX

In this Appendix, we shall determine where the zeros of the denominator  $D(s)$  lie for the case considered in Sec. IIB. The general formula for  $D(s)$  is

$$D(s) = (-ik_2 - \kappa_{2r})(\gamma_2 - ik_1) - i\gamma_1 k_1.$$

Here  $k_j$  may be written as

$$k_j = K_j e^{i\theta_j/2},$$

where  $K_j = |k_j|$ , and the angle  $\theta_j$  takes values on the four sheets as defined in (2.11). We examine whether it is possible for both  $\text{Re}D$  and  $\text{Im}D$  to vanish for points on the four sheets close to the real  $s$  axis in the vicinity of the threshold  $s_2$ .

Consider, for example, a point on sheet I lying above the segment  $s_1 < s < s_2$ . Its position can be specified by  $\theta_1 = 2\epsilon_1$ ,  $\theta_2 = \pi - 2\epsilon_2$ , where  $\epsilon_1$  and  $\epsilon_2$  are small and positive. Then, to first order in  $\epsilon_j$ ,

$$k_1 \approx K_1(1 + i\epsilon_1),$$

$$k_2 \approx iK_2(1 - i\epsilon_2),$$

and  $D(s)$  reduces to

$$D(s) \approx [(K_2 - \kappa_{2r})(\gamma_2 + \epsilon_1 K_1) + \epsilon_1 \gamma_1 K_1 - \epsilon_2 K_1 K_2] + i[(\kappa_{2r} - \gamma_1)K_1 - (K_1 + \epsilon_2 \gamma_2)K_2].$$

We see that  $\text{Im}D$  can vanish only if  $\kappa_{2r} > \gamma_1$ . Taking this to be the case, and substituting for  $K_2$  in  $\text{Re}D$ , we obtain

$$\text{Re}D = \{-\gamma_1 \gamma_2 K_1 - \epsilon_2 [\gamma_2^2 \kappa_{2r} + K_1^2 (\kappa_{2r} - \gamma_1)]\} / (K_1 + \epsilon_2 \gamma_2).$$

Obviously for  $\kappa_{2r} > \gamma_1$ ,  $\text{Re}D$  cannot vanish, and thus it is impossible to satisfy both  $\text{Re}D = 0$ ,  $\text{Im}D = 0$ .

Likewise, one can show that  $D(s)$  does not have a zero below the segment  $s_1 < s < s_2$  on sheet I.

Similar investigations may be carried out for points on the other three sheets. It may be easily deduced that poles close to the real axis in the region between the thresholds are impossible in sheet III as well as sheet I. However, for  $\kappa_{2r} < 0$ , there is a pole in sheet IV. As  $\kappa_{2r}$  becomes positive, it can be shown that this pole approaches the lower end of the inelastic cut, crosses over it at a point just above the branch point  $s_2$  and so passes into sheet II.<sup>29</sup> This is illustrated in Fig. 6 of the text. Unitarity is not violated in this process since, as seen in Fig. 4(b), a pole can move between sheet IV and sheet II without appearing on the physical sheet I.

<sup>29</sup> The authors wish to thank M. Nauenberg for valuable discussions and correspondence on this point.